technische universität
dortmund

Arbeit zur Erlangung des akademischen Grades
Bachelor of Science

Freeze-In Production of sterile Neutrino Dark Matter

Carlo Tasillo
geboren in Dortmund

2018

Lehrstuhl für Theoretische Physik III
Fakultät Physik
Technische Universität Dortmund

Erstgutachter:	Prof. Dr. Päs
Zweitgutachter:	Jun.-Prof. Dr. Brod
Abgabedatum:	11.07.2018

Kurzfassung

In dieser Arbeit wird die Freeze-In-Produktion Dunkler Materie untersucht, welche aus sterilen Neutrinos besteht. Das verwendete Modell basiert auf einem Standardmodell-Neutrino und einem sterilen Neutrino, welches über den Typ-I-Seesaw-Mechanismus die Masse des aktiven Neutrinos generiert. Die zum Prozess $h \to \bar{\nu}N$ zugehörige Boltzmann-Gleichung wird analytisch und numerisch gelöst, um den beobachteten Anteil $\Omega_{\mathrm{DM}} \simeq 0{,}258$ der kalten Dunklen Materie an der Energiedichte des Universums zu erklären. Es wird gezeigt, dass die dadurch möglichen sterilen Neutrinos eine Masse von $239{,}3\,\mathrm{keV}$ oder ca. $120\,\mathrm{keV}$ unter der Masse des Higgs-Bosons haben müssen. Außerdem wird gezeigt, dass beide Optionen jedoch aufgrund des Strahlungszerfalls $N \to \gamma\nu$ nicht als Erklärung für die gesamte Dunkle Materie dienen können.

Abstract

In this thesis, the freeze-in production of sterile neutrino dark matter is investigated in a model with one active and one sterile neutrino species which is expected to account for the active neutrino's mass due to the type I seesaw mechanism. The corresponding Boltzmann equation for the process $h \to \bar{\nu}N$ is solved analytically and numerically to yield the observed cold dark matter density $\Omega_{\mathrm{DM}} \simeq 0.258$. It is shown that the possible sterile neutrinos are expected to have a mass around $239.3\,\mathrm{keV}$ or about $120\,\mathrm{keV}$ below the Higgs mass. Eventually, both options are shown to be unfeasible because of the radiative decay $N \to \gamma\nu$.

Contents

1 Introduction

The standard model (SM) of particle physics is a quantum field theory developed in the latter half of the 20th century. Although it has achieved huge success by explaining three of the four fundamental interactions and various experimental observations, it is still far from being a complete theory of nature: two of its main problems are the evidence for dark matter (DM) and neutrino oscillations.

During the last few decades, strong evidence was found that there must be an as yet unknown type of matter, which is only observable by its gravitational interactions with ordinary matter. Even though DM accounts for about 80% of matter in the Universe and about 25% of its energy density, there is still no indication what DM might consist of on a particle level. The SM does not contain a particle species which could account for the measured effects in cosmology and astrophysics. However, the assumption that DM exists seems to be well-founded: The existence of halos of DM around galaxies would not only explain the often cited rotation curves of galaxies (see figure 1.1) and their stability, but also the observed effects of gravitational lensing of galaxy clusters as well as the angular power spectrum of the cosmic microwave background (CMB). The latter was measured by the space observatory Planck and provided a basis for our current standard model of cosmology, the concordance or Lambda-CDM model.

The SM states that all three currently assumed neutrino families are massless, which forbids a mixture between their flavor and mass eigenstates. This neutrino mixing was observed by several experiments, however, which were recognized with the Nobel Prize in Physics in 2015. Hence, we can no longer assume that neutrino masses vanish, but have to account for their tiny mass scale, which is millions of times smaller than that of other elementary particles. One theoretical concept for solving this is the seesaw mechanism. In its simplest version, the introduction of sterile, right-handed neutrino fields with suitable values for their Yukawa couplings and masses into the Lagrangian density of the SM yields a possibility to explain the order of magnitude of the neutrino masses. This might be less justified than the postulation of DM, since it postpones the problem of small neutrino masses to a lack of explanation for their Yukawa couplings and the newly introduced masses. Nevertheless, this argument can be weakened. If the additionally required Majorana mass terms in the Lagrangian density of the SM did not occur, a new physical

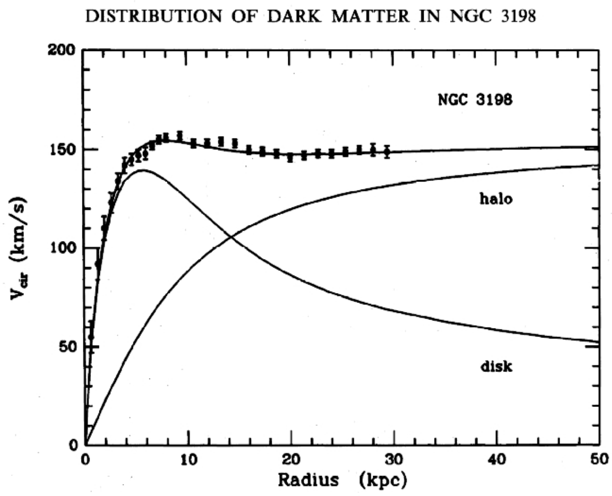

Figure 1.1: Characteristic flat rotation curve of the spiral galaxy NGC 3198 as measured by van Albada et al. in 1985 [1]. The graph labeled "disk" depicts the expected rotation curve if all of the galaxy's mass were accumulated in visible stars. The graph denoted by "halo" is a fit for the dark matter halo as a function of distance from the galaxy's center, needed to generate the observed rotation curve above.

law which forbids their existence would be needed. Therefore, the insertion of right-handed neutrinos appears to be better founded than previously thought.

An obvious question one has to ask after introducing these extra neutrinos into the SM is whether this extension can be used as a solution for other problems as well. This bachelor's thesis investigates the question if the type I seesaw mechanism can also explain the origin of dark matter. For the time being, this seems to be possible, given that right-handed neutrinos are massive, electrically uncharged and cosmologically stable. To simplify the model for a first survey, it is instrumental to reduce the number of active and sterile neutrino families to one and to solely consider the decay of the Higgs boson $h \to \bar{\nu}N$, where N denotes the right-handed neutrino.

2 Theoretical Background

The following section provides the theoretical background necessary for understanding the calculations and argumentation carried out in this bachelor's thesis and is based on the lecture "Cosmology, quantum cosmology and gravitational waves" held in the fall semester 2017 at TU Dortmund university. However, if not indicated differently, the listed definitions and reasoning can also be reviewed in most introductory pieces on cosmology, e.g. [2], while section 2.3 relies on [3] and section 2.5 relies on [4]. Throughout the calculations, natural units are used, in which $c = \hbar = k_\mathrm{B} = 1$.

2.1 The Concordance Model

The Lambda-CDM[1] or concordance model is currently the most accepted model of Big Bang cosmology, since it is the theory with the least number of parameters, able to explain the CMB anisotropies, the distribution of galaxies, the abundances of light elements and the accelerated expansion of the Universe. It is based on the cosmological principle, which states that the spatial distribution of matter is homogenic and isotropic when viewed on a large enough scale, and assumes that general relativity is the correct mathematical description for gravity. The cosmological principle is consistent with the highly isotropical CMB as measured by the Planck mission in 2016.

Solving the Einstein equations with these assumptions yields the Friedmann-Lemaître-Robertson-Walker (FLRW) metric:

$$\mathrm{d}s^2 = \mathrm{d}t^2 - a(t)^2 \left(\frac{\mathrm{d}r^2}{1 - \kappa r^2} + r^2 \mathrm{d}\Omega \right) . \tag{2.1}$$

The parameter $\kappa \in \{-1, 0, 1\}$ describes the curvature of space-time (referring to hyperbolic, Euclidean and elliptical space) and $a(t)$ is called the "scale factor", since it parameterizes the metric expansion of space.

[1] "Lambda-CDM" denotes the assumed existance of vacuum energy and cold dark matter.

It can be shown that the cosmological principle directly requires the energy-momentum tensor to take the form

$$(T^{\mu\nu}) = \mathrm{diag}(\rho, p, p, p) \tag{2.2}$$

at every point in space-time. Inserting this into the 00 component of the Einstein equations leads to the first Friedmann equation

$$H(t)^2 \equiv \left(\frac{\dot{a}(t)}{a(t)}\right)^2 = \frac{8\pi G}{3}\rho - \frac{\kappa}{a(t)^2}, \tag{2.3}$$

where $H(t)$ is the Hubble parameter, while the ij components lead to the second Friedmann equation

$$\frac{\ddot{a}(t)}{a(t)} = -\frac{4\pi G}{3}(\rho + 3p). \tag{2.4}$$

Using both of the Friedmann equations (2.3) and (2.4), it is easy to show a third useful relation

$$\dot{\rho} = -3H(t)(\rho + p) \tag{2.5}$$

and to conclude that the Universe must have been hot and dense at its beginning (often referred to as the “Big Bang”). Hence, it is appropriate to assume that in the early Universe the energy density ρ and the pressure p related to an equation of state corresponding to relativistic particles (i.e. radiation): $p = \frac{1}{3}\rho$. Substituting this condition into equation (2.5), one obtains

$$\rho_{\mathrm{radiation}} \propto a(t)^{-4}. \tag{2.6}$$

Integrating the first Friedmann equation (2.3), using this proportionality and neglecting the curvature term, leads to

$$H(t) = \frac{1}{2t}, \tag{2.7}$$

which will be used for the calculations in chapter 3.

The current Hubble parameter (called Hubble constant) H_0 is typically presented in units of the dimensionless constant h

$$H_0 = H(t_0) = 100h \, \frac{\mathrm{km}}{\mathrm{s\,Mpc}}, \tag{2.8}$$

and it is convenient to define the following parameters, where the sums over i imply a distinction between different kinds of matter or energy, i.e. radiation, vacuum energy as well as baryonic and dark matter:

$$\rho_{\mathrm{crit}}(t) \equiv \frac{3H(t)}{8\pi G} \tag{2.9}$$

$$\rho(t) \equiv \sum_i \rho_i(t) \tag{2.10}$$

$$\Omega_i(t) \equiv \frac{\rho_i(t)}{\rho_{\mathrm{crit}}(t)} \tag{2.11}$$

$$\Omega(t) \equiv \sum_i \Omega_i(t). \tag{2.12}$$

The cosmological parameters used in this thesis are the current dark matter density Ω_{DM}, the dimensionless Hubble constant h and the mean temperature T_0 of the CMB.

2.2 Thermodynamics of the Early Universe

In general, the number density for a certain particle species i with the degeneracy g_i in thermal equilibrium can be calculated by solving the following integral:

$$n_i^{\mathrm{eq}} = \frac{g_i}{(2\pi)^3} \int \mathrm{d}^3p \, f_i(\vec{p}), \tag{2.13}$$

where $f_i(\vec{p})$ is either the Fermi-Dirac or the Bose-Einstein distribution, depending on the spin of the particle species studied. The corresponding energy density can be calculated likewise:

$$\rho_i^{\mathrm{eq}} = \frac{g_i}{(2\pi)^3} \int \mathrm{d}^3p \, E_i(\vec{p}) f_i(\vec{p}). \tag{2.14}$$

When dealing with thermodynamics in the radiation-dominated era, all particle species are assumed to be relativistic, i.e. $T \gg m$, and to have vanishing chemical potentials. Solving the integral in equation (2.14) under these conditions yields

$$\rho_i^{\mathrm{R,\,eq}} = \frac{\pi^2}{30} g_i T^4 \times \begin{cases} 1 & \text{boson} \\ \frac{7}{8} & \text{fermion.} \end{cases} \tag{2.15}$$

It results that the total energy density of relativistic particles in the early Universe can be calculated by

$$\rho_{\mathrm{tot}}^{\mathrm{R,\,eq}} = \frac{\pi^2}{30} g_{\mathrm{eff}}(T)\, T^4, \tag{2.16}$$

where the effective degeneracy is given by

$$g_{\mathrm{eff}}(T) = \sum_{i\,=\,\mathrm{bosons}} g_i \left(\frac{T_i}{T}\right)^4 + \frac{7}{8} \sum_{i\,=\,\mathrm{fermions}} g_i \left(\frac{T_i}{T}\right)^4 . \tag{2.17}$$

In the time period investigated in this thesis, all particle species of the SM are still in thermal equilibrium and therefore have the same temperature T_i. Counting all of their degrees of freedom leads to $g_{\mathrm{eff}}(T \gtrsim m_t) = 106.25$, where m_t denotes the mass of the top quark, which is the first species to fall out of the thermal equilibrium at $T \simeq m_t$.

The entropy of a single particle species can be shown to be conserved and its entropy density is given by

$$s_i = \frac{\rho_i + p_i}{T_i}. \tag{2.18}$$

This yields the following total entropy density

$$s = \frac{2\pi^2}{45} g_{\mathrm{eff,\,s}}(T)\, T^3, \tag{2.19}$$

when summed over all particle species of the SM in a very good approximation until today, since the entropy is dominated by relativistic particles. The newly introduced quantity $g_{\mathrm{eff,\,s}}(T)$ is defined analogously to (2.17) as

$$g_{\mathrm{eff,\,s}}(T) = \sum_{i\,=\,\mathrm{bosons}} g_i \left(\frac{T_i}{T}\right)^3 + \frac{7}{8} \sum_{i\,=\,\mathrm{fermions}} g_i \left(\frac{T_i}{T}\right)^3 , \tag{2.20}$$

which also takes a value of $g_{\mathrm{eff,\,s}}(T \gtrsim m_t) = 106.25$ in the investigated time period. Its present-day value can be approximated as $g^0_{\mathrm{eff,\,s}} = 3.91$.

2.3 Generating Neutrino Masses with the Type I Seesaw Mechanism

As mentioned in the first chapter, evidence shows neutrinos must have mass, which is not included in the SM. Therefore, new mass terms have to be included into the Lagrangian density of the SM. The mass term generated by the Dirac Lagrangian (for any fermion field Ψ) is

$$\mathcal{L}_{\text{mass}}^{\text{Dirac}} = -\overline{\Psi} m \Psi = -\overline{\Psi}_{\text{L}} m \Psi_{\text{R}} - \overline{\Psi}_{\text{R}} m \Psi_{\text{L}}, \tag{2.21}$$

which is not gauge invariant under the electroweak symmetry group, since Ψ_{L} and Ψ_{R} behave differently under $\text{SU}(2)_L$ and $\text{U}(1)_Y$. This would directly lead to vanishing lepton masses as it is required that gauge freedom exists. However, this problem was solved by the Higgs mechanism. By introducing Yukawa couplings y_Ψ in a Lagrangian of the form

$$\mathcal{L}_{\text{Yukawa}} = -y_\Psi \overline{\Psi}_{\text{L}} h \Psi_{\text{R}} - y_\Psi \overline{\Psi}_{\text{R}} h \Psi_{\text{L}}, \tag{2.22}$$

which is gauge invariant, one is able to generate Dirac masses which do not violate the gauge freedom. When the Higgs field h receives a vacuum expectation value (VEV) v by spontaneous symmetry breaking, the Dirac mass of the fermion field Ψ amounts to $m_\Psi = y_\Psi v$:

$$\mathcal{L}_{\text{Yukawa}} = -\overline{\Psi}_{\text{L}} \underbrace{y_\Psi v}_{=m_\Psi} \Psi_{\text{R}} - \overline{\Psi}_{\text{R}} \underbrace{y_\Psi v}_{=m_\Psi} \Psi_{\text{L}}. \tag{2.23}$$

The Higgs mechanism turned out to be convincing for most of the lepton masses. Neutrino masses, however, are still fraught with problems in the SM, since a Dirac mass term would require right-handed neutrinos, which have not been observed yet. Another option would be a Majorana mass term

$$\mathcal{L}_{\text{mass}}^{\text{Majorana}} = -\frac{1}{2} \overline{\nu}_{\text{L}} m_{\text{LL}} \nu_{\text{L}}^c - \frac{1}{2} \overline{\nu}_{\text{L}}^c m_{\text{LL}} \nu_{\text{L}}, \tag{2.24}$$

where the exponent c denotes the CP conjugation of the respective field. Nevertheless, this mass term would violate both lepton number and gauge invariance and thus is forbidden.

A convenient solution to this problem is the type I seesaw mechanism. Its idea is to assume that the Majorana mass terms are generated effectively by introducing right handed neutrino fields ν_R. These fields are singlets under the SM gauge group, and couple with the active neutrinos. Hence, we are left with two possible terms, namely the Dirac mass term

$$-\overline{\nu}_\mathrm{L} m_\mathrm{LR} \nu_\mathrm{R} - \overline{\nu}_\mathrm{R} m_\mathrm{LR} \nu_\mathrm{L}, \tag{2.25}$$

and another Majorana mass term

$$-\frac{1}{2}\overline{\nu}_\mathrm{R} M_\mathrm{RR} \nu_\mathrm{R}^c - \frac{1}{2}\overline{\nu}_\mathrm{R}^c M_\mathrm{RR} \nu_\mathrm{R}. \tag{2.26}$$

This set of mass terms can be summarized in form of a mass matrix:

$$-\frac{1}{2}\begin{pmatrix}\overline{\nu}_\mathrm{L} & \overline{\nu}_\mathrm{R}^c\end{pmatrix}\begin{pmatrix}0 & m_\mathrm{LR}\\ m_\mathrm{LR}^\mathrm{T} & M_\mathrm{RR}\end{pmatrix}\begin{pmatrix}\nu_\mathrm{L}^c\\ \nu_\mathrm{R}\end{pmatrix} + h.c. \tag{2.27}$$

Diagonalizing this matrix and adopting the approximation that $M_\mathrm{RR} \gg m_\mathrm{LR}$ yields effective Majorana masses as defined in (2.24), which are naturally suppressed by the size of M_RR

$$m_\mathrm{LL} = -m_\mathrm{LR} M_\mathrm{RR}^{-1} m_\mathrm{LR}^\mathrm{T}. \tag{2.28}$$

The applied approximation is justified, since the mass scale of m_LR is thought to be the electroweak scale, while the newly introduced neutrinos are electroweak singlets and therefore not bound to this scale. In the case of only one active neutrino ν and one sterile neutrino N, equation (2.28) can be written in terms of one Yukawa coupling y, the Higgs VEV v and the right handed neutrino mass m_N

$$m_\nu = \frac{y^2 v^2}{m_N}. \tag{2.29}$$

In the last step, the sign of m_ν was dropped, owing to its absorption into the complex phase of the SM neutrino field.

2.4 Derivation of the Boltzmann Equation

Assuming there were no particle interactions, the total number of particles of a given species would be constant, which would result in the following relation for their number density n:

$$\frac{\mathrm{d}}{\mathrm{d}t}\left(na(t)^3\right) = 0 \quad\implies\quad \dot{n} + 3nH = 0. \tag{2.30}$$

Now considering that there actually are interactions $i_1 + ... + i_a \leftrightarrow i_{a+1} + ... + i_n$ that are able to change the species of the particles investigated, one has to include the following term

$$\begin{aligned}\dot{n} + 3Hn = -\int \mathrm{d}\mathcal{P}^n\, (2\pi)^4 \delta^{(4)} &\left(\sum_{i=1}^{a} p_i - \sum_{i=a+1}^{n} p_i\right) \\ \times &\left(|\mathcal{M}_{\rightarrow}|^2 \prod_{i=1}^{a} f_i - |\mathcal{M}_{\leftarrow}|^2 \prod_{i=a+1}^{n} f_i\right),\end{aligned} \tag{2.31}$$

where

$$\mathrm{d}\mathcal{P}^n = \prod_{i=1}^{n} \frac{g_i}{(2\pi)^3}\frac{\mathrm{d}^3 p_i}{2E_i} \tag{2.32}$$

is the Lorentz-invariant phase space, the $\delta^{(4)}$ term enforces the conservation of energy and momentum and the latter bracket represents the rate at which the process transforms the particles 1 to a into $a+1$ to n. This can be simplified by assuming that CP-symmetry is conserved, which is equivalent to saying that the forward and backward processes have the same squared transition amplitudes $|\mathcal{M}|^2 \equiv |\mathcal{M}_{\leftarrow}|^2 = |\mathcal{M}_{\rightarrow}|^2$. A further simplification can be adopted by approximating the distribution functions f_i by multiples α_i of the Boltzmann distribution f_i^{eq}:

$$f_i \equiv \alpha_i f_i^{\mathrm{eq}} = \alpha_i \mathrm{e}^{-E_i/T}\,,\ \text{where } \partial_{p_i}\alpha_i = 0. \tag{2.33}$$

Using energy conservation and equation (2.13) leads to

$$\dot{n} + 3Hn = -\gamma^{\mathrm{eq}}\left(\prod_{i=1}^{a}\frac{n_i}{n_i^{\mathrm{eq}}} - \prod_{i=a+1}^{n}\frac{n_i}{n_i^{\mathrm{eq}}}\right), \tag{2.34}$$

where

$$\gamma^{\mathrm{eq}} \equiv \int \mathrm{d}\mathcal{P}^n \, (2\pi)^4 \delta^{(4)} \left(\sum_{i=1}^{a} p_i - \sum_{i=a+1}^{n} p_i \right) |\mathcal{M}|^2 \prod_{i=1}^{a} f_i. \tag{2.35}$$

It is useful to exclude the effect of the expansion of the Universe so one can consider solely the evolution of the particle number density in a comoving volume. This can be done by defining the quantity $Y \equiv n/s$ and surmising that the number of effective degrees of freedom g_{eff} is approximately constant in the investigated time period, which yields

$$s\dot{Y} = -\gamma^{\mathrm{eq}} \left(\prod_{i=1}^{a} \frac{Y_i}{Y_i^{\mathrm{eq}}} - \prod_{i=a+1}^{n} \frac{Y_i}{Y_i^{\mathrm{eq}}} \right). \tag{2.36}$$

Finally, since it is common to express the quantities used rather as functions of temperature than as functions of time, one should introduce the dimensionless time parameter $z = m/T$, which fulfills the condition $\dot{z} = zH(z)$. The Boltzmann equation thus can be rewritten as

$$szH(z)Y' = -\gamma^{\mathrm{eq}} \left(\prod_{i=1}^{a} \frac{Y_i}{Y_i^{\mathrm{eq}}} - \prod_{i=a+1}^{n} \frac{Y_i}{Y_i^{\mathrm{eq}}} \right), \tag{2.37}$$

where Y' denotes the derivative of Y with respect to z.

2.5 Freeze-In and Freeze-Out Processes

As mentioned in section 2.2, massive particles did not remain in thermal equilibrium until today. If they did, the Universe would consist mostly of photons, since any massive particle density would be exponentially suppressed. To understand "the origin of species", as [2] puts it, it is crucial to investigate the deviations from equilibrium, that led to today's relic densities of massive particles. In general, there are two different kinds of basic processes that can lead out of the equilibrium: freeze-in and freeze-out processes. The following is intended to contrast both mechanisms in the case of DM relic densities.

Freeze-out mechanism: The DM is initially in thermal equilibrium and decouples from the heat bath, when the DM interaction rate drops below the Hubble parameter $H < \Gamma$. Or in other words: The thermal equilibrium cannot be sustained any longer, when the Universe expands so fast that the interactions which maintain the equilibrium are no longer efficient due to causality (typically at $z \sim 20$). The generated yield is characteristically proportional to the inverse square of the coupling strength λ: $Y_{\mathrm{FO}} \propto 1/\lambda^2$ (see figure 2.1).

Freeze-in mechanism: The DM has a negligible initial abundance, because of its feeble interaction with the thermal bath. As the Universe evolves, more of the so called FIMPs (Feebly Interacting Massive Particles) are produced by decaying particles from the bath, however still suppressed by the small coupling. When the temperature reaches the decaying particle's mass ($z \sim 1$), the process gets dominant and a yield that is proportional to the square of the coupling strength is produced: $Y_{\mathrm{FI}} \propto \lambda^2$ (see figure 2.1).

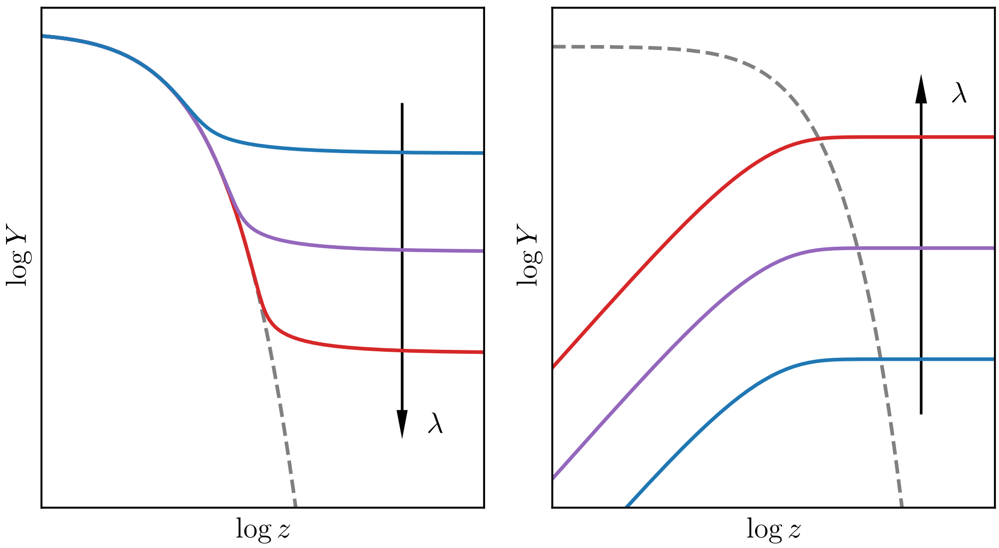

Figure 2.1: Two schematic log-log plots for the basic mechanisms of DM genesis: the conventional freeze-out (left) and the freeze-in (right) processes as a function of the dimensionless time parameter z for three different values of the coupling strength between the visible sector and DM particles. The dashed gray lines represent the equilibrium density of DM particles and the arrows indicate the effect of an increased coupling on the yield in each case.

3 Solutions of the Boltzmann Equation

3.1 The Boltzmann Equation for $h \to \bar{\nu} N$

To apply the Boltzmann equation in its general form (2.37) to the decay of the Higgs boson $h \to \bar{\nu} N$, one has to calculate the space-time density of the decay in thermal equilibrium γ^{eq}. By assuming that $|\mathcal{M}|^2$ does not depend on the relative motion of particles with respect to the plasma, the calculation yields

$$\gamma^{\text{eq}} = n_h^{\text{eq}} \mathit{\Gamma}_h \frac{\mathrm{K}_1(z_h)}{\mathrm{K}_2(z_h)}, \tag{3.1}$$

where K_i are the modified Bessel functions of the second kind, $\mathit{\Gamma}_h$ is the decay width of the Higgs boson in its rest frame [5] and $z_h = m_h/T$. Therefore the Boltzmann equation for this decay takes the following form

$$Y_h' = -\frac{\mathit{\Gamma}_h}{z_h H} \frac{\mathrm{K}_1(z_h)}{\mathrm{K}_2(z_h)} Y_h^{\text{eq}} \left[\frac{Y_h}{Y_h^{\text{eq}}} - \frac{Y_N}{Y_N^{\text{eq}}} \frac{Y_\nu}{Y_\nu^{\text{eq}}} \right]. \tag{3.2}$$

Given that both the Higgs boson and the active neutrino interact with the other SM particles in the thermal bath, one can assume that they stay in thermal equilibrium for the time period investigated. Hence, one can write $Y_h = Y_h^{\text{eq}}$ and $Y_\nu = Y_\nu^{\text{eq}}$ to get

$$Y_h' = -\frac{\mathit{\Gamma}_h}{z_h H} \frac{\mathrm{K}_1(z_h)}{\mathrm{K}_2(z_h)} Y_h^{\text{eq}} \left[1 - \frac{Y_N}{Y_N^{\text{eq}}} \right]. \tag{3.3}$$

To get a differential equation for the sterile neutrino density Y_N, a relation between Y_h' and Y_N' has to be found. Since it is expected that the creation of a sterile neutrino is directly linked to the annihilation of a Higgs boson and vice versa (at least in the early Universe), $Y_h' = -Y_N'$ seems to be a reasonable guess. We are left with

$$Y_N' = \frac{\mathit{\Gamma}_h}{z_h H} \frac{\mathrm{K}_1(z_h)}{\mathrm{K}_2(z_h)} Y_h^{\text{eq}} \left[1 - \frac{Y_N}{Y_N^{\text{eq}}} \right]. \tag{3.4}$$

Now, the equations (2.3) and (2.16) can be used to find the z_h dependence of the Hubble parameter

$$H(z_h) = \sqrt{\frac{8\pi^3}{90} g_{\text{eff}}} \frac{m_h^2}{m_{\text{pl}}} \frac{1}{z_h^2}, \tag{3.5}$$

where $m_{\text{pl}} \equiv \sqrt{\frac{\hbar c}{G}}$ is the Planck mass. To obtain the corresponding z_h dependence of $Y_h^{\text{eq}} \equiv n_h^{\text{eq}}/s$, the integral in equation (2.13) is solved at high energies for a boson with negligible chemical potential and mass m_h:

$$n_h^{\text{eq}} = \frac{g_h}{2\pi^2} \frac{m_h^3}{z_h} \mathrm{K}_2(z_h). \tag{3.6}$$

Using equation (2.19) yields

$$Y_h^{\text{eq}}(z_h) = \frac{45}{4\pi^4} \frac{g_h}{g_{\text{eff, s}}} z_h^2 \mathrm{K}_2(z_h). \tag{3.7}$$

A calculation analogous to that in (3.6) for Y_h^{eq} leads to the similar expression

$$Y_N^{\text{eq}} = \frac{45}{4\pi^4} \frac{g_N}{g_{\text{eff, s}}} \left(\frac{m_N}{m_h}\right)^2 z_h^2 \mathrm{K}_2\left(\frac{m_N}{m_h} z_h\right). \tag{3.8}$$

The last unknown quantity in equation (3.4) is the decay width Γ_h of the process $h \to \bar{\nu}N$. It can be calculated by solving the following integral [6]:

$$\Gamma_h = \frac{1}{2m_h} \int \frac{1}{2E_\nu} \frac{\mathrm{d}^3 p_\nu}{(2\pi)^3} \frac{1}{2E_N} \frac{\mathrm{d}^3 p_N}{(2\pi)^3} (2\pi)^4 \delta^{(4)}(p_h - p_\nu - p_N) \left|\mathcal{M}\right|^2, \tag{3.9}$$

which can be done by several substitutions leading to

$$\Gamma_h = \begin{cases} 0 & m_h \le m_\nu + m_N \\ \frac{|\vec{p}_N|}{8\pi m_h^2} \left|\mathcal{M}\left(|\vec{p}_N|\right)\right|^2 & m_h > m_\nu + m_N \end{cases} \tag{3.10}$$

where

$$|\vec{p}_N| = \frac{1}{2m_h}\sqrt{m_h^4 + m_\nu^4 + m_N^4 - 2m_h^2 m_\nu^2 - 2m_h^2 m_N^2 - 2m_\nu^2 m_N^2}. \tag{3.11}$$

The squared transition amplitudes with summation over initial and final spins $|\mathcal{M}|^2$ can be calculated by consulting the Feynman rules and Casimir's Trick for the occurring products of spinors. This leads to the following trace in Feynman slash notation, which can be transformed using the trace theorems for γ matrices:

$$\begin{aligned} |\mathcal{M}(|\vec{p}_N|)|^2 &= y^2 \mathrm{Tr}\left[(\not{p}_N + m_N)(\not{p}_\nu - m_\nu)\right] &(3.12)\\ &= 4y^2(p_N \cdot p_\nu - m_N m_\nu). &(3.13)\end{aligned}$$

Plugging in equation (3.11) and approximating $m_\nu \ll m_N$ yields

$$\Gamma_h = \frac{y^2 m_h}{8\pi}\left(1 - \frac{m_N^2}{m_h^2}\right)^2. \tag{3.14}$$

Finally, inserting equations (3.5), (3.7), (3.8) and (3.14) into (3.4) leads to the following result:

$$\begin{aligned} Y_N' &= \sqrt{\frac{90}{8\pi^3}}\frac{45}{32\pi^5}\frac{g_h}{g_{\text{eff, s}}\sqrt{g_{\text{eff}}}}\frac{y^2 m_{\text{pl}}}{m_h}\left(1-\frac{m_N^2}{m_h^2}\right)^2 z_h^3\,\mathrm{K}_1(z_h)\left[1-\frac{Y_N}{Y_N^{\text{eq}}}\right] &(3.15)\\ &= \sqrt{\frac{90}{8\pi^3}}\frac{45}{32\pi^5}\frac{g_h}{g_{\text{eff, s}}\sqrt{g_{\text{eff}}}}\frac{y^2 m_{\text{pl}}}{m_h}\left(1-\frac{m_N^2}{m_h^2}\right)^2 z_h^3\,\mathrm{K}_1(z_h) \\ &\times\left[1-\left(\frac{45}{4\pi^4}\frac{g_N}{g_{\text{eff, s}}}\left(\frac{m_N}{m_h}\right)^2 z_h^2\,\mathrm{K}_2\left(\frac{m_N}{m_h}z_h\right)\right)^{-1} Y_N\right]. &(3.16)\end{aligned}$$

3.2 Analytical Solutions of the Boltzmann Equation

The differential equation (3.16) has the following mathematical form

$$\frac{\mathrm{d}Y_N(z_h)}{\mathrm{d}z_h} = \alpha z_h^3\,\mathrm{K}_1(z_h)\left[1 - \frac{Y_N(z_h)}{\beta z_h^2\,\mathrm{K}_2(\gamma z_h)}\right] \quad \alpha,\beta,\gamma \in \mathbb{R}, \tag{3.17}$$

which is expected to not have any nontrivial analytical solutions. However, by assuming that $Y_N \ll Y_N^{\mathrm{eq}}$, equation (3.17) can be simplified to

$$\frac{\mathrm{d}Y_N(z_h)}{\mathrm{d}z_h} = \alpha z_h^3 \, \mathrm{K}_1(z_h), \tag{3.18}$$

which can be integrated to give a closed form solution for $Y_N(z_h)$. Further assuming that $Y_N(0)$ vanishes (see section 2.5) yields

$$Y_N(z_h) = \alpha \int_0^{z_h} \mathrm{d}x \, x^3 \, \mathrm{K}_1(x), \tag{3.19}$$

so that the present sterile neutrino abundance can be approximated as

$$Y_N^0 \equiv Y_N(z_h \to \infty) = \alpha \int_0^{\infty} \mathrm{d}x \, x^3 \, \mathrm{K}_1(x) = \frac{3\pi}{2}\alpha. \tag{3.20}$$

This directly leads to an analytic expression for the density parameter Ω_N defined in equation (2.12) for the introduced sterile neutrino species in dependence of its mass m_N and its Yukawa coupling y. Combining (2.9), (2.11) and (3.20), and supposing that (2.19) still holds today at $T = T_0$ and that the sterile neutrinos are non-relativistic in the present so that $\rho_N^0 = m_N n_N^0$, gives

$$\Omega_N \equiv \frac{\rho_N^0}{\rho_{\mathrm{crit}}^0} = \frac{1}{4\pi}\sqrt{\frac{90}{8\pi^3}} \frac{g_{\mathrm{eff,\,s}}^0}{g_{\mathrm{eff,\,s}}} \frac{g_h}{\sqrt{g_{\mathrm{eff}}}} \frac{y^2 m_N}{m_h m_{\mathrm{pl}}} \left(1 - \frac{m_N^2}{m_h^2}\right)^2 \frac{T_0^3}{H_0^2}. \tag{3.21}$$

Equating this with the observed quantity Ω_{DM} and solving for positive y yields the required Yukawa coupling y_{ana} for producing the DM density Ω_{DM} according to the analytical solution (3.20) of the Boltzmann equation:

$$y_{\mathrm{ana}} = 2\sqrt{\frac{2}{3}} \sqrt[4]{\frac{\pi^5}{5}} \sqrt{\frac{g_{\mathrm{eff,\,s}}}{g_{\mathrm{eff,\,s}}^0}} \frac{\sqrt[4]{g_{\mathrm{eff}}}}{\sqrt{g_h}} \sqrt{\frac{m_{\mathrm{pl}} m_h^5}{m_N}} \frac{\sqrt{\Omega_{\mathrm{DM}}}}{m_h^2 - m_N^2} \frac{H_0}{\sqrt{T_0^3}}. \tag{3.22}$$

Figure 3.1 includes a plot of this relation and the condition (2.29) for generating the neutrino mass m_ν in the seesaw mechanism, where the physical constants listed in table 3.1 have been used. The intersections of the depicted graphs can be interpreted as those combinations of the Yukawa coupling y and the sterile neutrino mass m_N that lead to the observed DM yield and the expected active neutrino mass m_ν. The determined parameters can be found in table 3.2.

Parameter	Value
g_h	4
g_{eff}	106.75
$g_{\text{eff, s}}$	106.75
$g^0_{\text{eff, s}}$	3.91
Ω_{DM}	0.258
h	0.678
T_0	2.7255 K
v	246 GeV
m_ν	0.1 eV
m_h	125.2 GeV
m_{pl}	1.221×10^{19} GeV

Table 3.1: List of the physical constants that were used to produce figure 3.1 [7].

y	m_N
6.3×10^{-10}	239.3 keV
4.5×10^{-7}	125.199 88 GeV

Table 3.2: Possible Yukawa couplings y and sterile neutrino masses m_N for generating the observed DM abundance Ω_{DM} and the expected active neutrino mass $m_\nu \sim \mathcal{O}(0.1\,\text{eV})$.

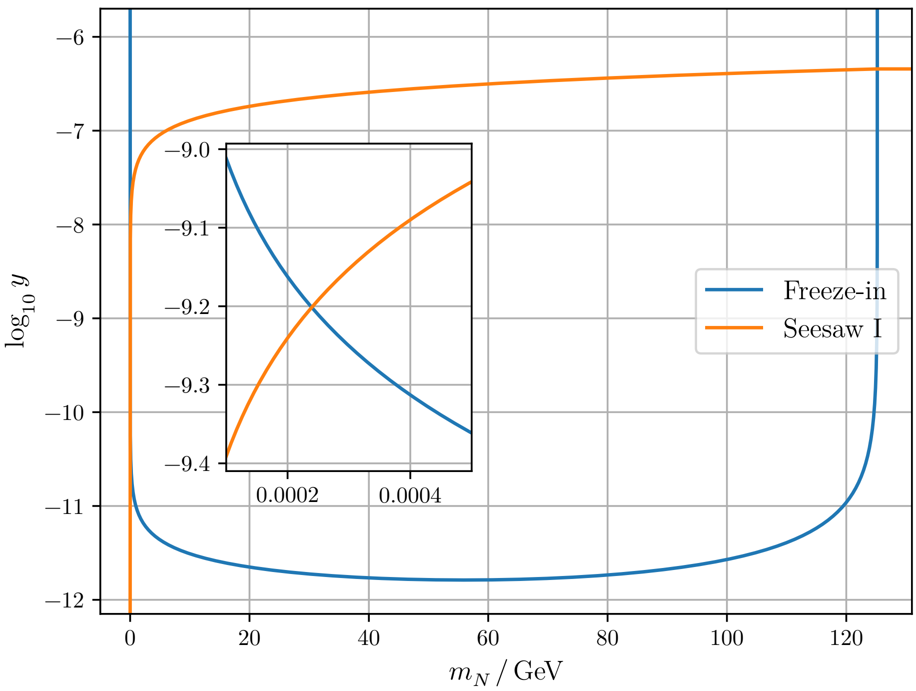

Figure 3.1: Plot of the relations (2.29) and (3.22) for generating the observed DM abundance $\Omega_{\mathrm{DM}} = 0.258$ and the expected active neutrino mass $m_\nu \sim \mathcal{O}(0.1\,\mathrm{eV})$. The intersections can be interpreted as the two possible combinations of y and m_N with which the active neutrino mass m_ν and the DM abundance Ω_{DM} can be realized in the model considered here. The parameters for these intersections are listed in table 3.2.

3.3 Numerical Solutions of the Boltzmann Equation

As previously stated, equation (3.16) is expected to not have any analytical solutions without the assumption $Y_N \ll Y_N^{\mathrm{eq}}$. Hence, a numerical solution of this differential equation is necessary to find exact predictions for y and m_N. The numerical stability can be improved by using the logarithmic representation of Y_N and z_h when calculating the derivative

$$\frac{Y_N}{z_h}\frac{\mathrm{d}\log Y_N}{\mathrm{d}\log z_h} = \sqrt{\frac{90}{8\pi^3}}\frac{45}{32\pi^5}\frac{g_h}{g_{\mathrm{eff,\,s}}\sqrt{g_{\mathrm{eff}}}}\frac{y^2 m_{\mathrm{pl}}}{m_h}\left(1-\frac{m_N^2}{m_h^2}\right)^2 z_h^3\,\mathrm{K}_1(z_h)$$
$$\times\left[1-\left(\frac{45}{4\pi^4}\frac{g_N}{g_{\mathrm{eff,\,s}}}\left(\frac{m_N}{m_h}\right)^2 z_h^2\,\mathrm{K}_2\left(\frac{m_N}{m_h}z_h\right)\right)^{-1} Y_N\right]. \qquad (3.23)$$

To find the necessary Yukawa coupling $y_{\mathrm{num}}(m_N)$ to produce the observed DM density, an algorithm is used which minimizes the difference between Ω_{DM} and the quantity

$$\Omega_N^{\mathrm{num}}(y, m_N) \equiv \frac{\rho_N^{0,\,\mathrm{num}}}{\rho_{\mathrm{crit}}^0} = \frac{16\pi^3}{135} g_{\mathrm{eff,\,s}}^0 \frac{m_N}{m_{\mathrm{pl}}^2}\frac{T_0^3}{H_0^2} Y_N^0(y, m_N) \qquad (3.24)$$

at a given m_N, where $Y_N^0(y, m_N)$ is the numerical solution of (3.23) at $z_h \gg 1$. The analytical expression (3.22) for $y_{\mathrm{ana}}(m_N)$ is used as an initial guess in each evaluation. Using the automated numerical solver for ordinary differential equations implemented in the software Mathematica [8] yields an output almost identical to that one represented in figure 3.1. The same physical parameters as in the analytical calculation (see table 3.1) and the initial and final values listed in table 3.3 are used for this cause.

Parameter	Value
$\log_{10} z_{h,\,\mathrm{init}}$	-20
$\log_{10} z_{h,\,\mathrm{fin}}$	10
$\log_{10} Y_N^{\mathrm{init}}$	-30

Table 3.3: List of the computational parameters that were used for the numerical solution of the Boltzmann equation (3.23).

To evaluate the deviation from the analytical results, the ratio $(y_{\text{num}} - y_{\text{ana}})/y_{\text{ana}}$ is calculated and plotted in dependence of m_N (see figure 3.2). It turns out that this ratio diverges at $m_N = 0$ and $m_N = m_h$, which is due to errors when calculating the numerical solution of the differential equation (3.23). However, the relative deviations in the regions around the two possible options of m_N that were obtained with the analytical approach are still remarkably small. For example, at $m_N = 239.3\,\text{keV}$ (see table 3.2), the analytical calculations yield $y_{\text{ana}} = 6.2884 \times 10^{-10}$ while the numerical result is $y_{\text{num}} = 6.2890 \times 10^{-10}$. This corresponds to a relative deviation of about 0.01%. Both calculations lead to the same result within the scope of an accuracy of at least 10 decimal places at $600\,\text{MeV} \lesssim m_N \lesssim 118\,\text{GeV}$.

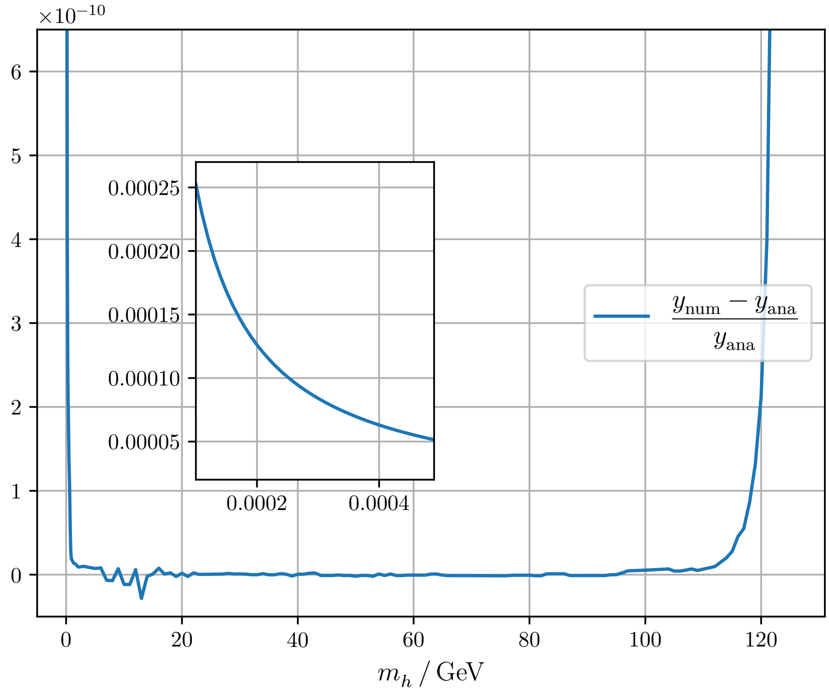

Figure 3.2: Plot of the relative deviation from the analytical calculations (3.22). Around $m_N = 239.3\,\text{keV}$ the deviation is only about 0.01% although the ratio plotted diverges at $m_N = 0$ and $m_N = m_h$.

To find the combinations of y_{num} and m_N with which the seesaw mechanism (2.29) additionally yields the active neutrino mass $m_\nu \sim \mathcal{O}(0.1\,\text{eV})$, another algorithm is implemented to find a local minimum of $|y_{\text{num}}(m_N) - y_{\text{seesaw}}(m_N)|$ close to a given m_N. Using the analytical findings for m_N as initial values confirms the parameters listed in table 3.2.

4 Discussion of the Results

4.1 Justification of the Assumptions

4.1.1 Derivation of the Boltzmann equation

For the derivation of (2.37), it was required that the effective number of degrees of freedom is constant for the time period investigated. This can be quantified by stating that the freeze-in of DM terminates at $z_h \sim 1$ (see next paragraph), which refers to a temperature of $T_{\mathrm{FI}} \sim m_h = 125.2\,\mathrm{GeV}$, corresponding to the elektroweak epoch, when $g_{\mathrm{eff}}(T \sim m_h) \approx 95.25$. Hence, the error made due to a changing effective number of degrees of freedom is of order $\mathcal{O}(10\%)$. However, since g_{eff} only occurs with exponents $-\frac{1}{2}$ and $\frac{1}{4}$ in (3.21) and (3.22), the error gets less significant.

4.1.2 Solution of the Boltzmann equation

The central assumption in the analytic solution in chapter 3.2 was that $Y_N(z_h) \ll Y_N^{\mathrm{eq}}(z_h)$. To demonstrate the accuracy of this claim, it is valuable to take a look at the occurring orders of magnitude of $Y_N(z_h)$ and Y_N^{eq}. Figure 4.1 depicts a plot of the analytical solution for the first combination of y and m_N in table 3.2. It can be seen that the equilibrium density Y_N^{eq} is more than three orders of magnitude higher than Y_N for the relevant period of time, in which the actual freeze-in happens ($z_h \sim 1$). As late as $z_h \sim 6$ the equilibrium density drops below the constant yield Y_N^0 and the assumption is not longer suitable. Nonetheless, at this time the freeze-in has already happened and a simplification of the differential equation is not necessary any more since its solution gets trivial. One can conclude that the analytical solution of the Boltzmann equation is therefore sufficiently exact and that the deviations depicted in figure 3.2 are dominantly due to numerical inaccuracies.

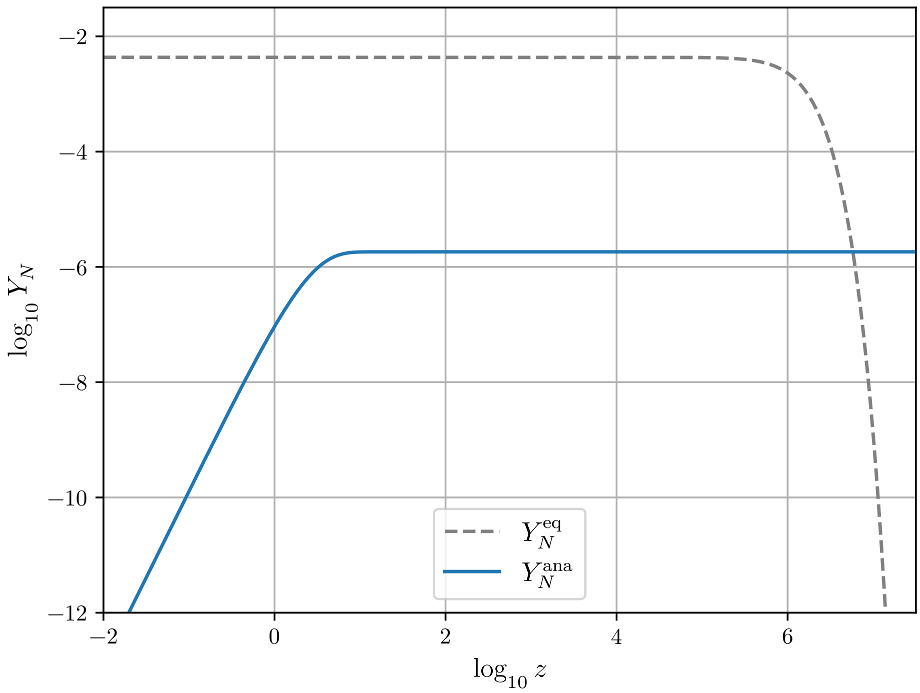

Figure 4.1: Exemplary plot to demonstrate the validity of $Y_N(z_h) \ll Y_N^{\mathrm{eq}}(z_h)$. The parameters of the first intersection in figure 3.1 were used to produce both graphs.

4.2 Physical Relevance of the Outcome

Both of the possible Yukawa couplings y (see table 3.2) are much smaller than unity, which in hindsight justifies the freeze-in approach to solve the Boltzmann equation. However, the problem of being unable to account for small active neutrino masses in the SM is postponed to the new issue of a lack of explanation for $y \ll 1$. This dilemma could be possibly solved in a more fundamental theory, though.

The Tremaine-Gunn bound is a fundamental criterion for fermionic DM candidates since it is simply a reformulation of the Pauli exclusion principle when applied to DM dominated galaxies. Experiments require a lower bound on sterile neutrino masses of 0.4 keV. Both of the possible masses m_N adhere to this condition. [9]

To count as a valid DM candidate, a particle species has to meet certain requirements. One of these criteria is the particle's stability on cosmological timescales which implies that its mean lifetime should exceed the age of the Universe. The strongest constraint on sterile neutrino DM is its radiative decay $N \to \gamma\nu$ into a photon and an active neutrino, for which the decay width can be approximated on one-loop level of the perturbation theory [10] to be

$$\Gamma_{N\to\gamma\nu} = \frac{9\alpha G_{\mathrm{F}}^2}{1024\pi^4} \sin^2(2\theta)\, m_N^5 \simeq 5.5 \cdot 10^{-22}\, \theta^2 \left(\frac{m_N}{\mathrm{keV}}\right)^5 \mathrm{s}^{-1}, \tag{4.1}$$

where $\alpha \simeq 1/137$, $G_{\mathrm{F}} \simeq 1.166 \times 10^{-5}\,\mathrm{GeV}^{-2}$, and the mixing angle is defined as

$$\theta \equiv \frac{m_\nu}{m_N}. \tag{4.2}$$

Putting in the obtained values for m_N yields the decay widths

$$\Gamma_{N\to\gamma\nu}(m_N = 239.3\,\mathrm{keV}) = 1.8 \times 10^{-16}\,\mathrm{s}^{-1} \tag{4.3}$$

$$\Gamma_{N\to\gamma\nu}(m_N = 121.199\,88\,\mathrm{GeV}) = 1.4 \times 10^{7}\,\mathrm{s}^{-1}, \tag{4.4}$$

which correspond to the following lifetimes

$$\tau_N(m_N = 239.3\,\mathrm{keV}) = 5.5 \times 10^{15}\,\mathrm{s} \tag{4.5}$$

$$\tau_N(m_N = 121.199\,88\,\mathrm{GeV}) = 7.4 \times 10^{-8}\,\mathrm{s}. \tag{4.6}$$

Since the age of the Universe is approximately $t_0 \approx 4 \times 10^{17}$ s, the sterile neutrino with a mass m_N slightly below the Higgs mass $m_h = 125.2\,\text{GeV}$ is definitely ruled out due to its instability, while the lifetime of the first sterile neutrino is only about 78 times too low to be called stable. Thus, a model with one active and one cosmologically stable sterile neutrino which accounts for the active neutrino's mass $m_\nu \sim \mathcal{O}(0.1\,\text{eV})$ by using the type I seesaw mechanism is not possible.

Nonetheless, the model can be adapted to comply with this constraint (next to others) when withdrawing the condition that only one DM particle species accounts for all of the observed DM abundance, and that there exists not only one active neutrino species, but three as in the SM. By introducing two other sterile neutrino species with individual Yukawa couplings and non-degenerate masses it could possible to explain all of the mass differences of the SM neutrinos and therefore the observed neutrino oscillations in addition to the current DM density. Additionally, if the lightest of the sterile neutrinos had a keV mass and the two heavy sterile neutrinos had masses in the range $150\,\text{MeV} \lesssim m_N^{2,3} \lesssim 100\,\text{GeV}$, a significant lepton asymmetry in the early Universe could have been generated. This could have resulted in today's baryon asymmetry. [9]

When trying to test the theory of these feebly interacting particle species, an enormous effort has to be put into the experimental tests since their direct detection seems to be hopeless. But there are still some possibilities to draw conclusions on the existence of sterile neutrino DM on an observational basis: The emitted photons of their radiative decay are often heralded as the "smoking gun" signal of sterile neutrino DM. The energy of these photons can be calculated using the aforementioned perturbation theory on one-loop level [9]:

$$E_\gamma = \frac{m_N}{2}\left(1 - \frac{m_\nu^2}{m_N^2}\right) \approx \frac{m_N}{2}. \tag{4.7}$$

Since the lightest sterile neutrino is expected to have a mass of several keV, the emitted photons would be observable in X-ray telescopes as a peak in the intensity at a given photon energy E_γ when observing structures in the Universe, where DM is believed to accumulate. Other observational evidence for sterile neutrino DM could be found in astrophysics, e.g. in the form of an explanation for several phenomena concerning supernovae. [10]

5 Summary and Perspective

The objective of this thesis was to investigate whether both the neutrino masses and the observed DM abundance could be explained with the freeze-in mechanism on the basis of a theory with only one active and one sterile neutrino. The arising Boltzmann equation could be solved analytically by assuming that the sterile neutrino number density in a comoving volume Y_N is much smaller than its equilibrium density Y_N^{eq} for a sufficiently large time period. This claim proved to be justified by solving the occurring differential equations without this assumption numerically, yielding the same results. Two possible combinations of the active neutrino's Yukawa coupling y and the sterile neutrino's mass m_N turned out to solve this problem. The first one corresponds to a right handed neutrino with a mass of $m_N = 239.3\,\mathrm{keV}$ and a Yukawa coupling $y = 6.3 \times 10^{-10}$ whose generated DM density can therefore be written by

$$\Omega_{\mathrm{DM}} h^2 \sim 0.12 \left(\frac{y}{6.3 \cdot 10^{-10}} \right)^2 \left(\frac{m_N}{239\,\mathrm{keV}} \right), \tag{5.1}$$

while the other one has a fine-tuned mass about $120\,\mathrm{keV}$ below the Higgs mass and a corresponding Yukawa coupling of $y = 4.5 \times 10^{-7}$. The latter case is definitely ruled out due to the decay $N \to \gamma\nu$, which yields an associated decay width of about $1.4 \times 10^7\,\mathrm{s}^{-1}$, whereas the first combination of values is more favorable for the condition of a particle species which is stable on cosmological timescales: This decay has a lifetime about 78 times smaller than the age of the Universe, which on the one hand is huge, but on the other hand not big enough to let the sterile neutrino be called “stable” in this context. Hence, the studied model with only one active and one sterile neutrino is not tenable.

However, if one drops the assumption of a simplified model with one SM and one right-handed neutrino, the radiative decay of the lightest sterile neutrino should become negligible on cosmological timescales due to a smaller required mass. Beyond that, the two additional sterile neutrinos could serve as an explanation for the observed neutrino oscillations by generating the mass differences between the active neutrino species. According to [9], a significant lepton number violation that could lead to the present baryon asymmetry can also be achieved under certain conditions. However, this would require a much more sophisticated theory that should also include oscillations of the active neutrinos into the sterile sector, which have been left out completely in this thesis along with an explanation for the smallness of the occurring Yukawa couplings. These open questions leave a vast space for further theoretical and experimental investigations which have yet to be carried out.

Bibliography

[1] Tjeerd van Albada et al. "Distribution of dark matter in the spiral galaxy NGC 3198". In: *The Astrophysical Journal* 295 (July 1985), pp. 305–313.

[2] E. Kolb and M. Turner. *The Early Universe*. Frontiers in physics. Avalon Publishing, 1994. ISBN: 9780813346458.

[3] M. Fukugita and T. Yanagida. *Physics of Neutrinos: And Applications to Astrophysics*. Springer, 2003. ISBN: 9783540438007.

[4] Nicolás Bernal et al. "The Dawn of FIMP Dark Matter: A Review of Models and Constraints". In: *Int. J. Mod. Phys.* A32.27 (2017), p. 1730023. DOI: 10.1142/S0217751X1730023X. arXiv: 1706.07442 [hep-ph].

[5] G. F. Giudice et al. "Towards a complete theory of thermal leptogenesis in the SM and MSSM". In: *Nucl. Phys.* B685 (2004), pp. 89–149. DOI: 10.1016/j.nuclphysb.2004.02.019. arXiv: hep-ph/0310123 [hep-ph].

[6] D. Griffiths. *Introduction to Elementary Particles*. Physics textbook. Wiley, 2008. ISBN: 9783527406012.

[7] M. Tanabashi et al. "Review of Particle Physics". In: *Phys.Rev.* D98 (2018), p. 030001.

[8] Wolfram Research Inc. *Mathematica, Version 11.3*. Champaign, IL, 2018.

[9] Alexey Boyarsky, Oleg Ruchayskiy, and Mikhail Shaposhnikov. "The Role of sterile neutrinos in cosmology and astrophysics". In: *Ann. Rev. Nucl. Part. Sci.* 59 (2009), pp. 191–214. DOI: 10.1146/annurev.nucl.010909.083654. arXiv: 0901.0011 [hep-ph].

[10] Alexander Kusenko. "Sterile neutrinos: The Dark side of the light fermions". In: *Phys. Rept.* 481 (2009), pp. 1–28. DOI: 10.1016/j.physrep.2009.07.004. arXiv: 0906.2968 [hep-ph].

Eidesstattliche Versicherung

Ich versichere hiermit an Eides statt, dass ich die vorliegende Abschlussarbeit mit dem Titel „Freeze-In Production of sterile Neutrino Dark Matter“ selbstständig und ohne unzulässige fremde Hilfe erbracht habe. Ich habe keine anderen als die angegebenen Quellen und Hilfsmittel benutzt, sowie wörtliche und sinngemäße Zitate kenntlich gemacht. Die Arbeit hat in gleicher oder ähnlicher Form noch keiner Prüfungsbehörde vorgelegen.

Ort, Datum	Unterschrift

Belehrung

Wer vorsätzlich gegen eine die Täuschung über Prüfungsleistungen betreffende Regelung einer Hochschulprüfungsordnung verstößt, handelt ordnungswidrig. Die Ordnungswidrigkeit kann mit einer Geldbuße von bis zu 50 000 € geahndet werden. Zuständige Verwaltungsbehörde für die Verfolgung und Ahndung von Ordnungswidrigkeiten ist der Kanzler/die Kanzlerin der Technischen Universität Dortmund. Im Falle eines mehrfachen oder sonstigen schwerwiegenden Täuschungsversuches kann der Prüfling zudem exmatrikuliert werden (§63 Abs. 5 Hochschulgesetz).

Die Abgabe einer falschen Versicherung an Eides statt wird mit Freiheitsstrafe bis zu 3 Jahren oder mit Geldstrafe bestraft.

Die Technische Universität Dortmund wird ggf. elektronische Vergleichswerkzeuge (wie z. B. die Software „turnitin“) zur Überprüfung von Ordnungswidrigkeiten in Prüfungsverfahren nutzen.

Die oben stehende Belehrung habe ich zur Kenntnis genommen.

Ort, Datum	Unterschrift